

**UCC Library and UCC researchers have made this item openly available.
 Please [let us know](#) how this has helped you. Thanks!**

Title	Structural and energetic origin of defects at the interface between germanium and a high-k dielectric from first principles
Author(s)	Elliott, Simon D.; Greer, James C.
Publication date	2011
Original citation	Elliott, S. D. and Greer, J. C. (2011) 'Structural and energetic origin of defects at the interface between germanium and a high-k dielectric from first principles', Applied Physics Letters, 98(8), pp. 082904. doi: 10.1063/1.3554703
Type of publication	Article (peer-reviewed)
Link to publisher's version	http://aip.scitation.org/doi/abs/10.1063/1.3554703 http://dx.doi.org/10.1063/1.3554703 Access to the full text of the published version may require a subscription.
Rights	© 2011 American Institute of Physics. This article may be downloaded for personal use only. Any other use requires prior permission of the author and AIP Publishing. The following article appeared in Elliott, S. D. and Greer, J. C. (2011) 'Structural and energetic origin of defects at the interface between germanium and a high-k dielectric from first principles', Applied Physics Letters, 98(8), pp. 082904 and may be found at http://aip.scitation.org/doi/abs/10.1063/1.3554703
Item downloaded from	http://hdl.handle.net/10468/4327

Downloaded on 2019-09-21T13:25:05Z

Structural and energetic origin of defects at the interface between germanium and a high- k dielectric from first principles

S. D. Elliott and J. C. Greer

Citation: *Appl. Phys. Lett.* **98**, 082904 (2011); doi: 10.1063/1.3554703

View online: <http://dx.doi.org/10.1063/1.3554703>

View Table of Contents: <http://aip.scitation.org/toc/apl/98/8>

Published by the [American Institute of Physics](#)



COMPUTING

ENGINEERING

SCIENCE

CiSE magazine is
an innovative blend.

computing
SCIENCE ENGINEERING
EXPLORING OUR
SOLAR SYSTEM

Structural and energetic origin of defects at the interface between germanium and a high- k dielectric from first principles

S. D. Elliott^{a)} and J. C. Greer

Tyndall National Institute, University College Cork, Lee Maltings, Cork, Ireland

(Received 10 September 2010; accepted 2 January 2011; published online 23 February 2011)

Atomic-scale models of the abrupt high- k /Ge interface with a range of suboxide stoichiometries GeO_x are presented and compared to their Si analogs. Molecular dynamics and geometry optimization were carried out at the density functional theory level to yield structures and energetics. Cohesion across the interface becomes stronger with increasing oxidation of the Ge suboxide. Three-coordinate Ge is identified as the main defect and is formed at low energetic cost, which accounts for the observed abundance of defects at oxide/Ge interfaces. The optimum low temperature interface is defect-free, predominantly Ge^{2+} with some Ge^+ . © 2011 American Institute of Physics. [doi:10.1063/1.3554703]

Relative to silicon (Si), germanium (Ge) has a higher mobility of electrons and holes, with the latter suggesting its use in future p-type metal-oxide-semiconductor transistors with high permittivity (k) dielectrics.¹ Ge suffers from a high density of electrically active defects at the interface to the dielectric.² We generate atomic-scale models for the abrupt interface between Ge (100) and a high- k dielectric and from these models predict the most abundant interfacial structure and defects.

Defect formation is likely to accompany oxidation of Ge—as computed recently for the Ge/ GeO_2 interface³—and is therefore linked to O content. Nevertheless, most models use arbitrary levels of O content. Band alignment was studied using a Ge/ GeO_2 interface model of fixed O content⁴ generated from its Si analog, based on a model of Si^+-Si^+ at an Si/tridymite- SiO_2 interface.⁵ A similar interface structure was shown to have Ge oxidation states in fair agreement with x-ray photoelectron spectroscopy,⁶ and a Ge dangling bond was introduced by the removal of bridging oxygen.⁷ The predicted energy of defect states is sensitive to the theoretical approach and structural model used.⁷⁻⁹ Bulk⁹ and interface³ models provide evidence that these defects cannot be hydrogen passivated and are not paramagnetic, although paramagnetic defects are observed in electrically detected magnetic resonance spectroscopy.¹⁰

The subject of this letter is the abrupt interfacial layer (IL) between Ge (100) and the high- k dielectric HfSiO_4 , building on a previous study on Si.¹¹ The simulation cell contains four semiconductor atoms in each (100) plane and is fixed at the optimum dimensions for the bulk crystal (59.0 \AA^2 for Si and 66.6 \AA^2 for Ge). By construction, the O content of the IL is $8x$ per cell, $0 \leq x \leq 1$ (i.e., zero to eight O atoms per cell) and the overall IL stoichiometry is GeO_{2x} , although after optimization the Ge suboxide is distributed over multiple layers. Outer semiconductor and high- k surfaces were terminated with H and OH, respectively, and separated by 13 \AA of vacuum ($\text{Hf}_4\text{Si}_4\text{Ge}_{40}\text{O}_{18+8x}\text{H}_{12}$ per cell). Non-spin-polarized total electronic energies were calculated using the Perdew Burke Ernzerhof (PBE) exchange-correlation functional¹² and a projected augmented wave de-

scription of cores,^{13,14} as implemented in VASP.^{15,16} The plane wave cutoff was 400 eV and reciprocal space was spanned by a $3 \times 3 \times 1$ k-point mesh. After ~ 5 ps of molecular dynamics with constrained H, the original high- k structure was reinstated and the atomic positions were optimized freely. All geometries were found to be stable in tests on larger cells. We define nondefective Ge atoms as those coordinated to four atoms (to $\pm 10\%$ of bulk bond lengths) and determine the formal oxidation state by counting the number of bonds to O. Undercoordinated Ge (“2 coor” and “3 coor”) is defined as a structural defect (Fig. 1).

For a given level of O content (x), our calculations yield similar optimized IL structures on Si and Ge. Most optimized structures show a single O atom bridging the suboxide and high- k layers perpendicular to the interface (e.g., Ge–O–Hf). The suboxide structure is complex but consistently shows two types of structures. One features Ge–Ge dimers at the interface to Ge^0 , as on bare Ge (100) surfaces;¹⁷ the other type is undimerized because O has been inserted into this bond (Ge–O–Ge). Having obtained various structural isomers from the calculations, we focus on the lowest energy structures of each type (Table I).

Relative energies are calculated using grand canonical thermodynamics, which is routinely used for oxide surfaces¹⁸ and was pioneered for interfaces in Ref. 11:

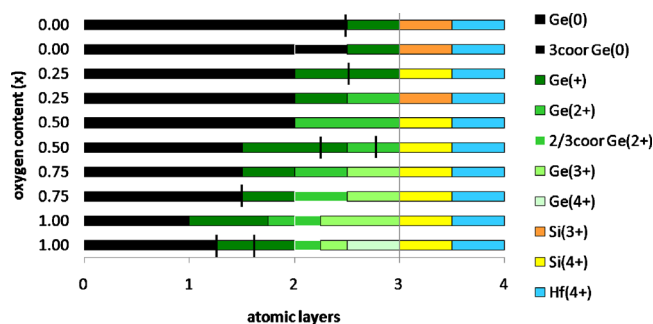


FIG. 1. (Color online) Layer-by-layer distribution of formal oxidation states computed for high- k /Ge interface at various levels of oxygen content. Vertical lines show the states involved in Ge–Ge dimers.

^{a)}Electronic mail: simon.elliott@tyndall.ie.

TABLE I. Computed data for abrupt HfSiO₄/Ge interfaces. At each level of O content (x), the lowest energy dimerized and undimerized interfaces are described by the amount of substoichiometric Ge oxide per ML of substrate (Fig. 1). Energetics indicate IL stability (ΔG_{IL} for vacuum annealing, Fig. 2) and, where applicable, the cost (ΔE) of forming defects at each value of x , which is used to estimate relative defect concentrations using $\exp(-\Delta E/k_{\text{B}}T)$.

x	Suboxide IL (ML)	ΔG_{IL} (J/m ²)	Defects (ML)	ΔE (eV/defect)	Rel. conc.
0.00	Ge _{0.5} Si ³⁺ _{0.5}	0.73	None	0.0	1
	Ge _{0.5} Si ³⁺ _{0.5}	1.40	(3 coor Ge ⁰) _{0.50}	1.38	10 ⁻⁶
0.25	GeO _{0.5}	0.08	None		
	Ge _{1.0} O _{0.5} Si ³⁺ _{0.5}	0.28	None		
0.50	GeO	-0.78	None		
	Ge _{1.5} O	-0.68	None		
0.75	Ge _{1.5} O _{1.5}	-1.20	None	0.0	0.99
	Ge _{1.5} O _{1.5}	-0.99	(2/3 coor Ge ²⁺) _{0.5}	0.44	0.01
1.00	Ge ₂ O ₂	-1.54	(3 coor Ge ²⁺) _{0.25}	0.0	0.99
	Ge _{1.5} O ₂	-1.43	(2 coor Ge ²⁺) _{0.25}	0.50	0.01

$$\begin{aligned} \Delta G_{\text{IL}} = & E(\text{slab}) - N(\text{H}_2\text{O})\mu(\text{H}_2\text{O}) - N(\text{GeH}_4)\mu(\text{GeH}_4) \\ & - N(\text{HfSiO}_4)\mu(\text{HfSiO}_4) - N(\text{Ge})\mu(\text{Ge}) \\ & - 4x\mu(\text{O}_2) - \Delta G_{\text{surf}}(\text{Ge} - \text{H}), \end{aligned} \quad (1)$$

where N is the number of units in the slab and μ is the chemical potential per unit calculated for molecules (H₂O, GeH₄, and O₂) or bulk crystals (HfSiO₄ and Ge). Since all slabs have identical bottom faces, the associated constant offset $\Delta G_{\text{surf}}(\text{Ge}-\text{H})=0.3$ J/m² can be estimated and subtracted. Using Eq. (1), the effect of O content on ΔG_{IL} can be determined for any partial pressure of oxygen, but we focus on vacuum annealing at $p(\text{O}_2)=10^{-9}$ atm and $T=700$ K.

The trend is for interfacial binding to become stronger (ΔG_{IL} more negative) with increasing O content at the IL (Table I). Ignoring the kinetics of O diffusion, there is a thermodynamic driving force toward oxidation even under O-poor conditions. This eventually yields layers of stoichiometric oxide between two interfaces (e.g., Ge/GeO₂/high- k).

As our interest is the minimum thickness of interfacial oxide, we examine metastable structures at $x < 1$. Graphs of ΔG_{IL} for both Si and Ge (Fig. 2) show concave kinks at $x=0.5$, where the IL oxidation energy (i.e., the slope of ΔG_{IL} versus x) changes from greater than to less than that of the bulk semiconductor. For example, from $x=0.25$ to $x=0.5$, ΔG_{IL} changes by -3.6 eV per Ge in the topmost monolayer (ML), while from $x=0.5$ to $x=0.75$ this change is -1.8 eV/Ge, compared to -2.1 eV for bulk $\text{Ge} \rightarrow \text{GeO}_2$ (dashed line). Rearrangement of O within the IL drives the system toward $x=0.5$. If the real system contains domains with various O stoichiometries and the total O content is constant, it is thermodynamically favorable to exchange O between domains to maximize the proportion of $x=0.5$.

We predict the most abundant substoichiometric IL to have O content $x=0.5$. Two structures are isoenergetic to 0.1 J/m² (0.1 eV/Ge at IL) at this stoichiometry. The structure in Fig. 3(a) shows each Ge at the IL coordinated to two substrate atoms and to two O atoms, i.e., nondimerized Ge²⁺ ML, which facilitates orientation of the O-bridge between suboxide and high- k layers along [100]. The structure in Fig. 3(b) shows Ge⁺-Ge⁺ and Ge²⁺-Ge²⁺ dimers, with the latter linked to sublayer Ge⁺ via O backbonds. It is important to

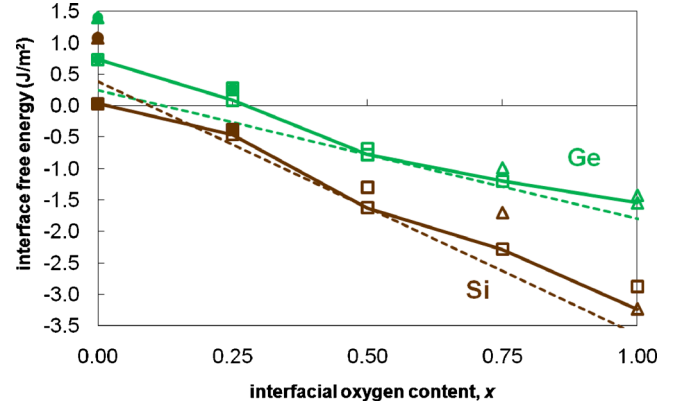


FIG. 2. (Color online) Energetics as a function of O content under annealing at $p(\text{O}_2)=10^{-9}$ atm for Ge (green, $T=700$ K) and Si (brown, $T=1200$ K). Some interfaces include defective Si/Ge (triangles), while others are entirely undefective (squares), and filled symbols indicate reduced Si cations in the high- k layer. Solid lines linking the minima show the trend in oxidation energy; the dashed lines show the trend for bulk $(1-x)\text{Si}+x\text{SiO}_2$ or $(1-x)\text{Ge}+x\text{GeO}_2$, offset so as to coincide with the respective minima at $x=0.5$.

note that IL structures at each value of x are local minima, with kinetic barriers toward the interconversion of one IL into another. In general then, the IL obtained in experiment depends sensitively on the conditions of substrate preparation, high- k growth, and annealing.

The data for $x < 1$ in Table I and Fig. 2 show that ILs with structurally defective Ge/Si are less stable than undefective ILs. At $x=0$, a nondimerized IL with half a ML of 3 coor Ge⁰ is about $\Delta E=0.7$ J/m² (1.4 eV per 3 coor Ge⁰) less stable than the dimerized version of exclusively four-coordinate Ge. The energy difference for similar Si structures

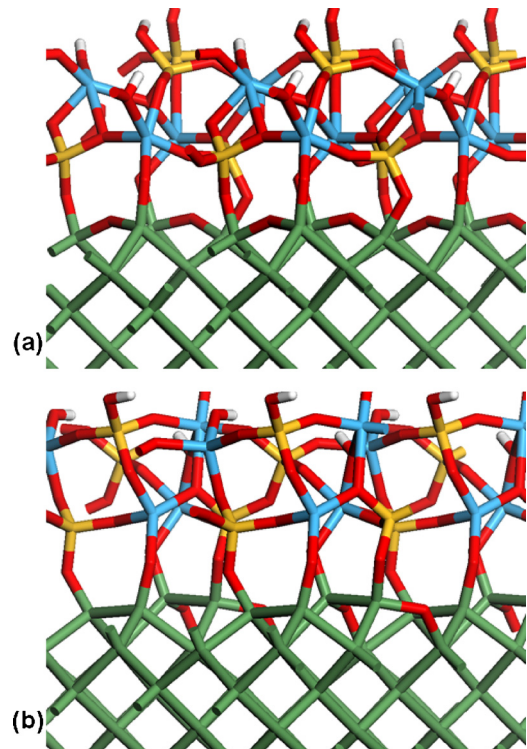


FIG. 3. (Color online) Computed atomic structures of the (a) undimerized and (b) dimerized HfSiO₄/Ge interfaces at $x=0.5$ that are predicted to predominate if O supply is limited (white=H, red/dark-gray=O, blue/pale-gray=Hf, yellow/pale-gray=Si, and green/mid-gray=Ge).

is $\Delta E = 1.0 \text{ J/m}^2$. Forming dimers at $x = 0.75$ leads to half a ML of defects, which increases the interfacial energy by $\Delta E = 0.2 \text{ J/m}^2$ and $\Delta E = 0.6 \text{ J/m}^2$ for Ge and Si, respectively. These energetics show that undercoordinated Si is significantly less stable than undercoordinated Ge, probably due to the tendency for Si to hybridize as sp^3 rather than s^2p^2 .

Assuming simplistically that just these two isomers exist for each value of x , we estimate their relative concentration at annealing temperatures (Table I). For instance, at $x = 0.75$, the dimerized IL with 3 coor Ge²⁺ and 2 coor Ge²⁺ defects is 0.4 eV per defect less stable than the undefective IL, so that equilibrium should yield a concentration of 1% defects at $x = 0.75$. This is many orders of magnitude more abundant than the corresponding Si defects. As noted above, thermodynamics alone cannot predict the proportion of $x = 0.75$ relative to other values of x , apart from arguing for $x = 0.5$ to be favored. It is however encouraging that fitting gives a reasonable value: 10% of $x = 0.75$ would mean 10^{11} defects/cm² (based on 6×10^{14} Ge/cm²), which is the defect density measured at Ge/GeO₂ interfaces.^{2,19} Hydrogen passivation may change their energetics, but this is thought not to be efficient for dangling bond defects in Ge.^{3,9}

The data show that structural defects can be healed or created by dimerization. Each Ge–Ge dimer bond can be viewed as “storing” an electron pair and reducing the number of bonds to O, which has the effect of healing defects when O-deficient ($x = 0$) or creating them when O-rich ($x = 0.75$). Oxidation by insertion of O into the Ge⁺–Ge⁺ dimer bond at $x = 0.25$ is a direct pathway to Ge²⁺–O–Ge²⁺, the most favored IL ($x = 0.5$). The data also demonstrate the complexity of defect energetics: Creating O-vacancies may initially produce undercoordinated Ge, but our simulations show that adequate perturbation and relaxation may restore a nondefective IL. Indeed, undercoordinated Ge can result from an *increase* in O content (e.g., if dimers are preserved). Therefore, a single formation energy for O vacancies at the interface cannot be defined, but a reasonable average value would be the reduction energy of the bulk, i.e., $\frac{1}{2}\text{GeO}_2 \rightarrow \frac{1}{2}\text{Ge} + \text{O}$.

The most common defect in these models is pyramidal 3 coor Ge. The unpaired electron (“dangling bond”) of undercoordinated Ge may be saturated by the addition of one more electron, reducing the effective oxidation state on Ge by one, as previously found for bulk Ge.⁹ Consistent with this, the neutral slabs were computed to be stable with respect to spin-polarization (i.e., diamagnetic), but the formation of other charge states was not tested here. Thus, Ge bound to three O atoms and to no Ge is designated as 3 coor Ge²⁺ ($x = 0.75$ and $x = 1$, Table I). The electron pair in the empty site is visible in the electronic structure as a high-lying valence band state in the IL. A similar defect was found in simulations of interface oxidation.³ We also find a 3 coor Ge⁰ defect bound to one O and two Ge ($x = 0$), but not bonded to the high- k layer above (2.9 Å from Hf). Direct coordination of O to three-coordinate defects is not seen in the most abundant defects at Si(100)/SiO₂ (namely, P_{b0} and P_{b1}),²⁰ which perhaps explains the higher defect abundance and resistance to passivation observed in the Ge case. Another defect that arises in the O-rich models is 2 coor Ge²⁺ with no dangling

bond ($x = 0.75$ and $x = 1$), where Ge is connected like an elbow to two O and no Ge. The computed ΔE at $x = 1$ suggests that it costs more energy to form 2 coor Ge²⁺ than 3 coor Ge²⁺. The well-known failings of standard density functionals in describing conduction band states prevent us from making quantitative predictions about the electrical behavior of the interface, such as band offsets, defect levels, charge trapping, and magnetic state

In summary, we used density functional theory to model abrupt high- k /Ge interfaces with a range of stoichiometries. Interfacial bonding is due to single O anions bridging the high- k and suboxide layers, becoming stronger with increasing oxidation of the suboxide. Under conditions where the supply of external O is limited, e.g., at low temperature, an optimum suboxide is obtained, consisting of both undimerized Ge²⁺O and dimerized Ge⁺Ge²⁺_{0.5}O. Structurally defective Ge arises naturally in some models but can be removed by making/breaking Ge–Ge dimers. Similar structures are obtained for Si, but with dramatically different energetics: Oxidation of the Ge interface yields about half as much energy and defective Ge is more abundant, with an estimated concentration consistent with experiment. The dominant defect is three-coordinate Ge²⁺ or Ge⁰, bound to at least one O.

This work was funded by Science Foundation Ireland under Grant Nos. 06/IN.1/I857 and 07/SRC/I1172 (“FORME”). The authors wish to acknowledge the SFI/HEA Irish Centre for High-End Computing (ICHEC) for the provision of computational facilities and support.

¹C. O. Chui, S. Ramanathan, B. B. Triplett, P. C. McIntyre, and K. C. Saraswat, *IEEE Electron Device Lett.* **23**, 473 (2002).

²H. Statz, L. Davis, Jr., and D. A. deMars, *Phys. Rev.* **98**, 540 (1955).

³L. Tsetseris and S. T. Pantelides, *Appl. Phys. Lett.* **95**, 262107 (2009).

⁴P. Broqvist, J. F. Binder, and A. Pasquarello, *Appl. Phys. Lett.* **94**, 141911 (2009).

⁵A. Ourmazd, D. W. Taylor, J. A. Tentschler, and J. Bevk, *Phys. Rev. Lett.* **59**, 213 (1987).

⁶G. Pourtois, M. Houssa, A. Delabie, T. Conard, M. Caymax, M. Meuris, and M. M. Heyn, *Appl. Phys. Lett.* **92**, 032105 (2008).

⁷M. Houssa, G. Pourtois, M. Caymax, M. Meuris, M. M. Heyns, V. V. Afanas'ev, and A. Stesmans, *Appl. Phys. Lett.* **93**, 161909 (2008).

⁸P. Broqvist, A. Alkauskas, and A. Pasquarello, *Mater. Sci. Semicond. Process.* **11**, 226 (2008).

⁹J. R. Weber, A. Janotti, P. Rinke, and C. G. Van de Walle, *Appl. Phys. Lett.* **91**, 142101 (2007).

¹⁰S. Baldovino, A. Molle, and M. Fanciulli, *Appl. Phys. Lett.* **96**, 222110 (2010).

¹¹S. Monaghan, J. C. Greer, and S. D. Elliott, *Phys. Rev. B* **75**, 245304 (2007).

¹²J. P. Perdew, K. Burke, and M. Ernzerhof, *Phys. Rev. Lett.* **77**, 3865 (1996).

¹³P. E. Blöchl, *Phys. Rev. B* **50**, 17953 (1994).

¹⁴G. Kresse and D. Joubert, *Phys. Rev. B* **59**, 1758 (1999).

¹⁵G. Kresse and J. Furthmüller, *Comput. Mater. Sci.* **6**, 15 (1996).

¹⁶G. Kresse and J. Furthmüller, *Phys. Rev. B* **54**, 11169 (1996).

¹⁷H. J. W. Zandvliet, *Phys. Rep.* **388**, 1 (2003).

¹⁸M. W. Finnis, A. Y. Lozovoi, and A. Alavi, *Annu. Rev. Mater. Res.* **35**, 167 (2005).

¹⁹D. Kuzum, T. Krishnamohan, A. J. Pethe, A. K. Okyay, Y. Oshima, Y. Sun, J. P. McVittie, P. A. Pianetta, P. C. McIntyre, and K. C. Saraswat, *IEEE Electron Device Lett.* **29**, 328 (2008).

²⁰A. Stirling, A. Pasquarello, J.-C. Charlier, and R. Car, *Phys. Rev. Lett.* **85**, 2773 (2000).